Arthropod Structure & Development 58 (2020) 100968

Contents lists available at ScienceDirect

Arthropod Structure & Development

journal homepage: www.elsevier.com/locate/asd

The origin of microscopic spheres on the exoskeleton of the woodlouse *Porcellionides pruinosus* (Crustacea: Isopoda) and their effect on its hydrophobicity

Miloš Vittori*, Ivana Gantar

Department of Biology, Biotechnical Faculty, University of Ljubljana, Večna Pot 111, SI-1000, Ljubljana, Slovenia

ARTICLE INFO

Article history:
Received 6 May 2020
Accepted 11 June 2020
Available online xxx

Keywords:
SEM
TEM
Oniscidea
Epicuticle
Ecdysis

ABSTRACT

The dorsal surface of the woodlouse *Porcellionides pruinosus* is covered with minute spheres, providing its characteristic powdered appearance. Little has been known about their composition and formation. A previously suggested function of these structures was to increase the hydrophobicity of the cuticular surface. We studied the ultrastructure, composition and formation of the spheres as well as tested whether they affect the hydrophobicity of the cuticle. We determined the composition of the spheres with histochemistry and scanning electron microscopy after applying various chemicals. We studied the process of their formation with transmission electron microscopy and assessed the hydrophobicity of the cuticle by measuring contact angles of water droplets with its surface. Our results show that the spheres are largely organic. They contain proteins and glycoproteins or possibly polysaccharides without detectable amounts of lipids. By studying the formation of the spheres we established that they are epicuticular structures. They are deposited early in the premolt stage of the molt cycle around branching extensions of epidermal cells. The sphere-covered cuticle of *P. pruinosus* is more hydrophobic than the cuticle with experimentally removed spheres as well as the scale-covered cuticle in a related species.

1. Introduction

Terrestrial isopods or woodlice (Oniscidea) are a group of crustaceans that have successfully colonized dry land, diversifying into more than 3700 known terrestrial and amphibious species (Sfenthourakis and Taiti, 2015). The isopod body is covered by a cuticle which represents an exoskeleton. In various species of woodlice, the surface of the cuticle forms diverse structures, including a variety of scales, setules and ridges (Schmalfuss, 1975; 1977; 1978; Vittori and Štrus, 2017). In the woodlouse *Porcellionides pruinosus* the dorsal surface is covered by microscopic spheres (Schmalfuss, 1978), which provide this species with its characteristic powdered appearance (Hadley and Hendricks, 1985).

Initially, the spheres were suggested to be waxy secretions (Schmalfuss, 1978). This was later disputed due to the inability of nonpolar solvents, such as hexane, to remove the spheres from the surface of the exoskeleton. However, their composition remained unknown, as they were not removed by any other treatment either to which they were subjected. These included aqueous acetic acid and potassium hydroxide solutions (Hadley and Hendricks, 1985). It has recently been shown that the spheres can be retained in paraffin sections and that they stain with the periodic acid-Schiff histological stain, indicating that they contain polysaccharides (Csonka et al., 2018).

It has previously been observed that freshly molted individuals are more pruinose than individuals that are about to molt. This suggested that the deposition of the spheres is molt-related. It was proposed that the spheres in *P. pruinosus* are formed immediately after molt by deposition from the molting fluid. This fluid still covers the tergites for a short time after molt (Hadley and Hendricks, 1985). Nevertheless, the exact time and mechanism of their formation remained unknown. Possibilities include secretion by glands, deposition from the molting fluid or deposition by epidermal cells during the premolt stage. Other surface ornamentation in woodlice, such as the epicuticular scales and tricorn sensilla, are deposited by epidermal cells at the same time as the rest of the epicuticle (Price and Holdich, 1980; Štrus et al., 2019; Vittori et al., 2012).

* Corresponding author.
E-mail address: milos.vittori@bf.uni-lj.si (M. Vittori).

https://doi.org/10.1016/j.asd.2020.100968

The process of molt in isopods is biphasic. During the first phase — the posterior molt — they shed the old cuticle of the body segments posterior to the fourth pereonite. After a brief interval — the intramolt stage — the cuticle of the cephalothorax and the anterior four pereonites is shed in the anterior molt. The premolt stage, during which woodlice secrete their new epicuticle and exocuticle, begins with apolysis, the detachment of the epidermis from the old cuticle. Apolysis creates the ecdysial space between the epidermis and the old cuticle. Terrestrial isopods are known to deposit mineral in the ecdysial space of the anterior four pereonites during the premolt stage in the form of sternal $CaCO_3$ deposits, which are resorbed during the intramolt stage (Ziegler et al., 2005). The formation of sternal deposits makes the animals in the premolt stage easily recognizable and facilitates the staging of their progression through this stage (Vittori et al., 2012; Zidar et al., 1998).

The function of the spheres on the surface of *P. pruinosus* is also unknown, but several authors have given it consideration. Schmalfuss (1978) suggested that the spheres could function in keeping the animals clean by making the surfaces of their cuticles hydrophobic. This would prevent the adhesion of soft particles and debris. An alternative explanation was that the spheres might help to minimize water loss across the cuticle. This would be beneficial as the species inhabits dry habitats (Hadley and Hendricks, 1985; Schmalfuss, 1978), yet it possesses only small amounts of lipids in its exoskeleton (Hadley and Warburg, 1986; Quinlan and Hadley, 1983).

In this study, we aimed to determine at which point in the molt cycle and by which mechanism the spheres are deposited as well as to shed more light on their composition. In addition, we attempted to test whether they affect the wettability of the cuticle.

2. Materials and methods

2.1. Laboratory culture and molt cycle stage determination

Woodlice were collected in Slovenia. Specimens of *P. pruinosus* originated from gardens near Cerknica (45°42′52″N 14°28′07″E) and Ajdovščina (45°56′27″N 13°44′08″E). Specimens of *Porcellio scaber* were collected in Črnomelj (45°34′05″N 15°11′18″E). Woodlice were kept in a climatic chamber at 21 °C and a 16 h photoperiod in plastic containers with soil from the sampling site and hazel (*Corylus avellana*) leaf litter as food. Premolt substages in *P. pruinosus* were determined on the basis of sternal $CaCO_3$ deposit development according to the staging system developed for *P. scaber* by Zidar et al. (1998). This approach distinguishes three substages of the premolt stage: PE1 ($CaCO_3$ deposits on individual sternites are in the form of separate patches), PE2 ($CaCO_3$ deposits of each sternite are fused) and PE3 ($CaCO_3$ deposits cover entire sternites). Specimens in the intramolt stage, i.e. after the molt of the posterior body half, were recognized by direct observation of the posterior molt.

2.2. Histochemical staining of paraffin sections

For the preparation of paraffin sections, animals were fixed with 4% aqueous formaldehyde at 4 °C overnight and incubated in a 10% aqueous solution of ethylenediaminetetraacetic acid (EDTA; pH 7.5) for 48 h to remove mineral from the exoskeleton. Samples were dehydrated in an ascending series of ethanol, cleared with xylene, infiltrated with paraffin wax (Paraplast Plus, Sigma–Aldrich) at 60 °C and embedded using the paraffin embedding station HistoCore Arcadia H (Leica). Paraffin sections 7 μm thick were prepared with an RM2265 microtome (Leica).

Histological staining with Weigert's iron hematoxylin and eosin (Kiernan, 1990), Alcian blue and eosin (Kiernan, 1990), periodic acid-Schiff (PAS) stain (Kiernan, 1990), ninhydrin-Schiff stain (Bancroft and Gamble, 2008) and mercuric bromophenol blue (Subramoniam, 1982) was performed in two parallels. For the PAS and ninhydrin-Schiff stains, sections incubated in the Schiff reagent without pretreatment were used as controls. Stained sections were dehydrated, cleared with xylene and mounted in Pertex (Medite).

2.3. Histochemical staining of frozen sections

For the demonstration of lipids, tergites were fixed in a mixture of 2% paraformaldehyde and 2.5% glutaraldehyde in 0.1 M HEPES buffer (pH 7.3) overnight at 4 °C and decalcified as described for paraffin sections. After removing EDTA with deionized water, samples were embedded in Tissue freezing medium® (Leica). Cryosections 16 μm thick were cut on a CM1850 cryostat (Leica) at −20 °C. Sections were transferred to poly-L-lysine coated microscope slides and dried. Staining was performed with Oil red O (Kim et al., 2015) and Sudan black (Kiernan, 1990). Control slides were incubated overnight in a mixture of methanol and chloroform (2:1 volume ratio) to remove lipids before staining.

2.4. Autofluorescence of the integument and fluorescence imaging

Whole-mount fluorescence imaging of the old cuticle and the ecdysial space was performed on tergites isolated from premolt stage individuals. Dissected tergites were fixed in methanol and mounted on glass slides in glycerol. We determined that spheres and tricorns are strongly autofluorescent under UV excitation (Supplementary material), which facilitated the fluorescence imaging of these structures. Imaging was performed with an AxioImager Z.1 microscope equipped with an ApoTome system for structured illumination imaging and an AxioCam MRm camera using Axiovision software (all from Zeiss). Stacks of optical sections were depth color coded with Fiji software using the plugin Temporal-Color Code (Schindelin et al., 2012).

2.5. Transmission electron microscopy (TEM)

For the preparation of resin sections, tissues were fixed and decalcified as described for histological staining of cryosections, postfixed with 1% aqueous osmium tetroxide and embedded in Agar 100 resin (Agar Scientific). Ultrathin sections (70 nm) were cut with a diamond knife (Diatome) using an Ultracut S ultramicrotome (Reichert) and collected on copper grids. Serial sections were collected on formvar-coated slot grids. Sections were contrasted with uranyl acetate and lead citrate and observed with a CM 100 transmission electron microscope (Philips) equipped with the cameras BioScan 792 and Orius SC200 (both from Gatan).

2.6. Scanning electron microscopy (SEM)

Tergites from *P. pruinosus* specimens were dissected and fixed in a mixture of 2% paraformaldehyde and 2.5% glutaraldehyde in 0.1 M HEPES buffer (pH 7.3) overnight at 4 °C. Specimens were postfixed with 1% aqueous osmium tetroxide for 2 h, dehydrated in an ascending concentration series of ethanol and air-dried in hexamethyldisilazane (HMDS). Dry samples were attached to aluminum holders using adhesive carbon discs and sputter coated with platinum. The old cuticle of individuals in the premolt stage was fractured with a needle to expose the ecdysial space.

For the determination of the effects of different chemical treatments, individual tergites from the pereons of three nonmolting animals were dissected without subsequent fixation. Care was taken to avoid hemolymph from contaminating the tergal surfaces during dissection. Tergites from each animal were treated

with 4% NaOCl at 21 °C for 2 h and 72 h, chloroform at 60 °C for 30 min, absolute methanol at 21 °C for 72 h or 10% aqueous EDTA at 21 °C for 72 h. Treatments were terminated by rinsing the tergites with three changes of 0.1 M HEPES buffer (pH 7.3). After rinsing, tergites were dehydrated and prepared for SEM as described for non-treated specimens. An additional set of tergites was left untreated as control. These tergites were air-dried immediately after dissection, attached to holders, sputter-coated with platinum and imaged with SEM. All SEM images were obtained with a JSM-7500F field emission scanning electron microscope (JEOL).

2.7. Wettability measurements

The wettability of powdered and non-powdered tergites was assessed and compared by measuring the contact angle, i.e. the angle between the solid–air and the liquid–air interfaces in water droplets of identical volumes (Hsu et al., 2011; Nosonovsky, 2007). To this end, woodlice were killed by decapitation and glued to glass slides with cyanoacrylate glue (Uhu). To remove the spheres, tergites of immobilized *P. pruinosus* individuals were stroked gently with filter paper until they no longer appeared powdered. For the measurements of contact angles, 1 μL droplets of deionized water were deposited on the tergites with a pipette (Eppendorf). Droplets were imaged from the side with a DigiMicro Profi digital microscope (DNT). Contact angles were measured on micrographs using Fiji software. Surfaces of powdered specimens of *P. pruinosus* (N = 48), *P. pruinosus* specimens with spheres removed (N = 18) and specimens of *P. scaber* (N = 20), were analyzed. In *P. scaber*, the tergites are covered with epicuticular scales and not with spheres. A sample of the analyzed specimens was then left to dry for 3 days, after which they were detached from the slides, transferred to brass holders, sputter coated with platinum and observed with SEM to assess the success of sphere removal. Pairwise comparisons between the analyzed groups were performed with the Mann–Whitney U test with Bonferroni corrected p-values using the software PAST (Hammer et al., 2001).

Fig. 1. (A) The woodlouse, *Porcellionides pruinosus*. Scale bar = 2 mm. (B) An individual that has just completed the anterior molt.

3. Results

3.1. Structuring of the dorsal surface in P. pruinosus

The dorsal body surface and the uropods of *P. pruinosus* reflect incident light, resulting in the pruinose appearance characteristic of these animals (Fig. 1). As revealed by microscopic observation, the powdery coating is made up of spheres ranging in size from just under 1 μm to about 4 μm (Fig. 2A–C). In addition to the spheres, flat rings of similar material are present on the tergites, raised slightly above the surface (Fig. 2). The outer diameter of the rings is 15–20 μm and they are 1–5 μm thick (Fig. 2A and D). They may be located separately, but they are most often positioned posteriorly to tricorn sensilla in groups of 1–4 rings per tricorn (Fig. 2A).

On undamaged tergites, spheres are arranged in a regular pattern of spheres which increase in diameter in successive rows in the posterior direction. This pattern is then periodically repeated (Fig. 2B). Each sphere is connected to the surface of the cuticle by a stalk about 500 nm long and 100–200 nm thick (Fig. 2C). The rings are also connected to the cuticle surface by a series of stalks similar to those attaching the spheres (Fig. 2D). Three types of surfaces are present on individual spheres: densely arranged round indentations just over 100 nm in diameter; winding ridges, which are spaced 100–150 nm apart; and smooth regions (Fig. 2C). The distal surfaces are smooth in larger spheres, which are more than 2 μm in diameter, whereas smaller spheres lack smooth patches. Similar surface patterning is evident on the rings (Fig. 2D). Their proximal surface is patterned into densely arranged round indentations identical to the structuring of the spheres, whereas their distal surface is smooth. In addition to the spheres, granules with a diameter of 50 nm cover the cuticular surface (Fig. 2C).

It is evident in cross-section that the spheres are outgrowths of the epicuticle (Fig. 2E). They are filled with inhomogeneous electron-dense material without cavities and covered by a distinct, 10 nm thick surface layer (Fig. 2E, inset). The stalks of the spheres also contain electron dense material that is rooted in the inner epicuticle while the surface layer of the stalks is continuous with the outer epicuticle (Fig. 2E).

Occasionally, circles of spheres are present instead of the typical rings. Alternatively, rings may be only partially formed, appearing as semicircles continuing into a series of circularly arranged spheres (Fig. 2F). In fact, a variety of transitions between circles of spheres and complete rings can be found on the tergites, particularly along their anterior edges (Fig. 2F).

3.2. Composition of the spheres

3.2.1. Histochemistry

When stained with the routine hematoxylin-eosin stain, the spheres stain strongly with eosin, but not with hematoxylin (Fig. 3A). In the remainder of the cuticle, the endocuticle stains only with eosin, while the exocuticle binds hematoxylin. The high affinity of the exocuticle for the mordant dye hematoxylin indicates that this region contains negatively charged macromolecules. Eosin, which stains the spheres, is an acidic dye, binding to

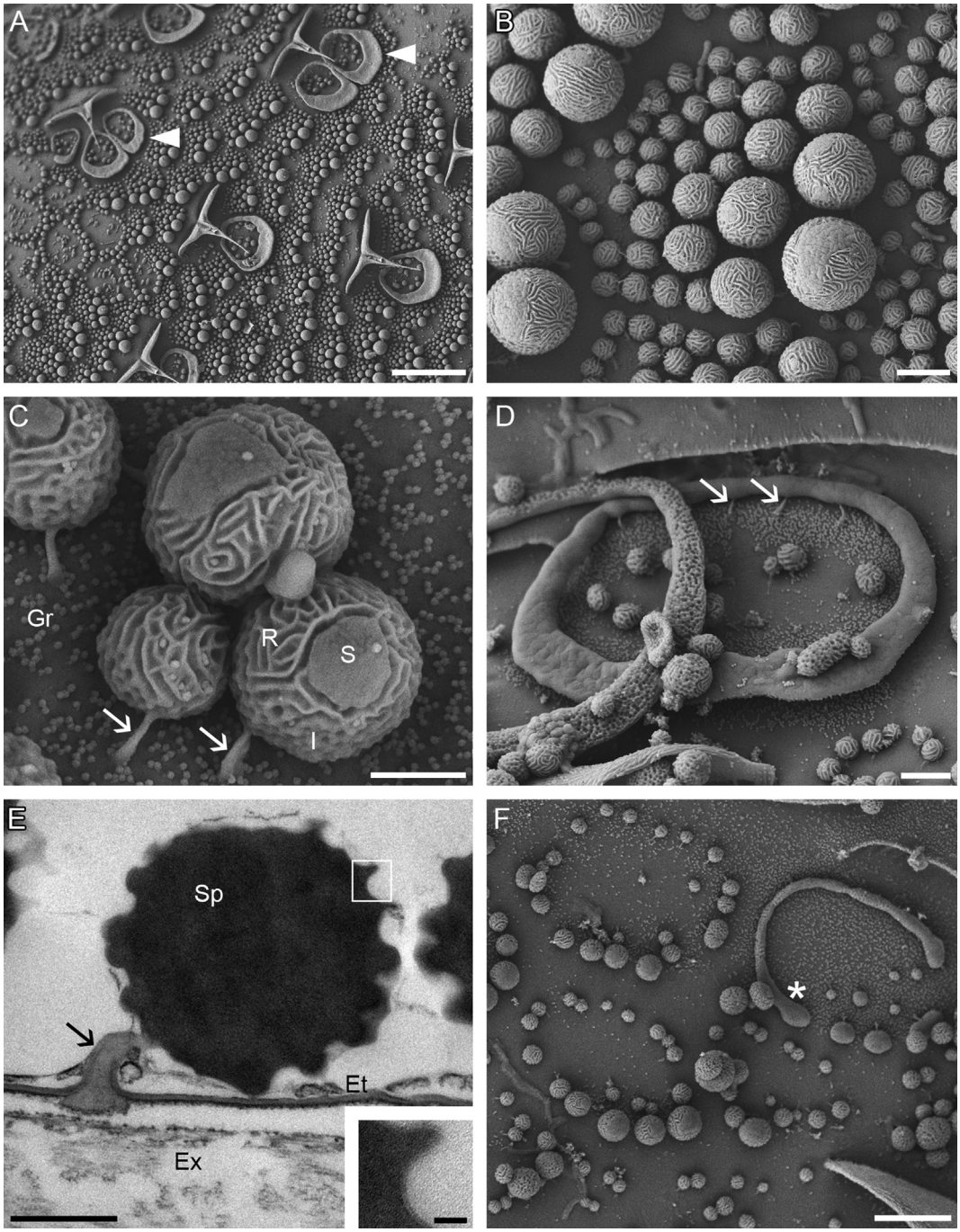

Fig. 2. Structures on the dorsal surface of *Porcellionides pruinosus*. (A) Scanning electron micrograph of the tergal surface, densely covered in a periodical pattern of spheres with increasing diameters. Rings (arrowheads) are visible posteriorly to tricorn sensilla. Scale bar = 10 μm. (B) Higher magnification image of the pattern of spheres. Scale bar = 2 μm. (C) The spheres are connected to the surface via stalks (arrows). Areas of their surfaces may be smooth (S) or structured, forming either ridges (R) or round indentations (I). Much smaller granules (Gr) cover the surface of the cuticle. Scale bar = 1 μm. (D) Rings on the surface have several stalks (arrows) and are smooth distally, whereas their proximal surface forms round indentations. These are visible on the detached ring on the left, which is flipped over. Scale bar = 2 μm. (E) Transmission electron micrograph of a sphere (Sp) in cross-section. The stalk (arrow) of the electron dense sphere extends from the epicuticle (Et). The surface layer of the stalk is continuous with the outer epicuticle and the material in its interior with the electron dense inner epicuticle. The white rectangle shows the position of the inset. Ex: exocuticle; scale bar = 0.5 μm. Inset: Higher magnification image showing the surface layer covering the spheres. Scale bar = 50 nm. (F). Scanning electron micrograph of the anterior edge of a tergite, showing rings of spheres and a partially fused ring (*), continuing as a row of spheres. Scale bar = 5 μm.

positively charged macromolecules. These are mostly positively charged amino acid residues of proteins in animal tissues. With Alcian blue, a cationic dye that stains macromolecules with high densities of negative charge, a weak staining of the exocuticle is visible while the spheres and the endocuticle do not stain. This pattern of staining is similar to that of hematoxylin (Fig. 3B). The staining of the exocuticle indicates greater amounts of negatively charged molecules in this region, particularly in the distal exocuticle, which stains more intensely.

With bromophenol blue, an acidic dye that stains proteins intensely, albite not specifically, the endocuticle is almost colorless. The exocuticle stains light blue and the spheres stain intensely,

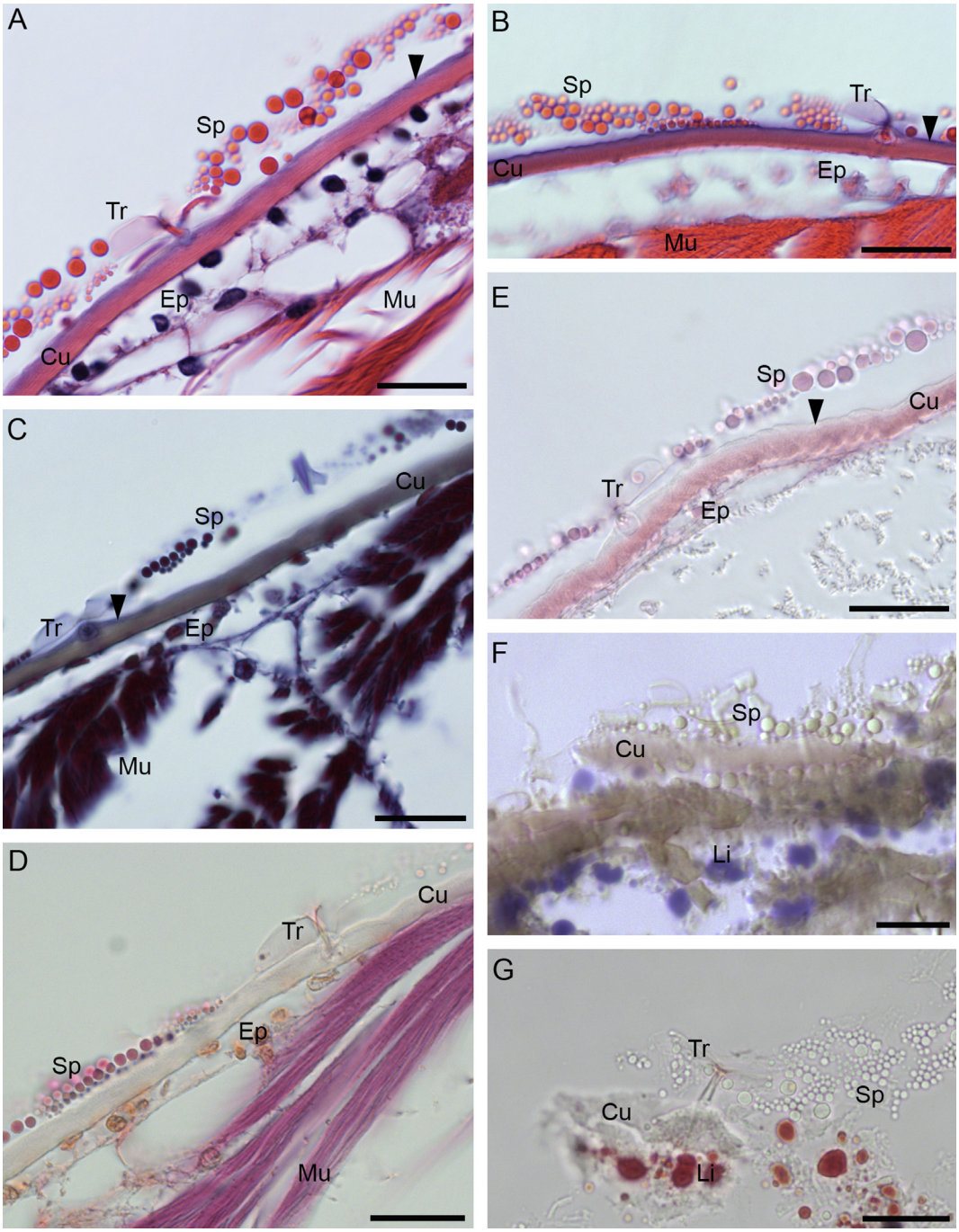

Fig. 3. Histological staining of spheres. (A) Paraffin section stained with hematoxylin and eosin. (B) Paraffin section stained with Alcian blue and eosin. (C) Paraffin section stained with bromophenol blue. (D) Paraffin section stained with the ninhydrin-Schiff stain. (E) Paraffin section stained with the periodic acid-Schiff stain. (F) Frozen section stained with Sudan black. (G) Frozen section stained with Oil red O. Arrowheads: exocuticle, Ep: epidermis, Cu: cuticle, Li: lipid droplets, Mu: muscle tissue, Sp: spheres, Tr: tricorn sensilla. Scale bars = 20 μm.

similar to muscle cells in the underlying tissues (Fig. 3C). The presence of large amounts of protein in the spheres is further indicated by their intense staining with the ninhydrin-Schiff stain, which specifically stains primary amino groups and can thus highlight the presence of proteins. With this stain, the endocuticle stains weakly, the exocuticle slightly more strongly and the spheres very strongly, comparable in intensity to the muscle tissue in the same section (Fig. 3D).

With the PAS stain, which is specific for carbohydrates, the endocuticle stains strongly, the exocuticle weakly and the spheres relatively strongly (Fig. 3E). The staining of the endocuticle can be attributed to chitin, which is known to be present in the cuticle, or to glycosylated proteins. The staining of the spheres indicates that they contain either polysaccharides or glycosylated proteins as both are stained with the PAS reaction.

In cryosections, the spheres stain with neither Oil red O nor Sudan black. The staining with these dyes was localized to lipid droplets in the epidermis while the cuticle remained unstained (Fig. 3F and G). The spheres thus do not contain lipids, at least not in demonstrable amounts.

3.2.2. Chemical exposure experiments

The surface of control tergites prepared without fixation appears very similar to fixed tergites (Fig. 4A). Decalcification of the tergites with the chelating agent EDTA results in the removal or flattening of the small granules, but does not appear to affect the morphology of the spheres (Fig. 4B). It is therefore unlikely that the spheres contain large amounts of calcium minerals. The granules, on the other hand, might contain a greater proportion of mineral. Incubations in methanol (Fig. 4C) or hot chloroform (Fig. 4D) do not alter the appearance of the spheres, confirming that they do not contain large amounts of soluble lipids. Treatment with an aqueous solution of NaOCl for 2 h results in the spheres appearing deflated, resembling collapsed sheets of material attached to the cuticle by stalks (Fig. 4E). This shows that their interior is rapidly degraded while their surface remains largely intact after this treatment. Incubation in aqueous NaOCl for 72 h completely removes most spheres as well as the epicuticle, revealing the underlying mineralized exocuticle and small holes where the spheres previously attached (Fig. 4F). Only a few completely flattened remnants of spheres can still be visible on the surface following such treatment.

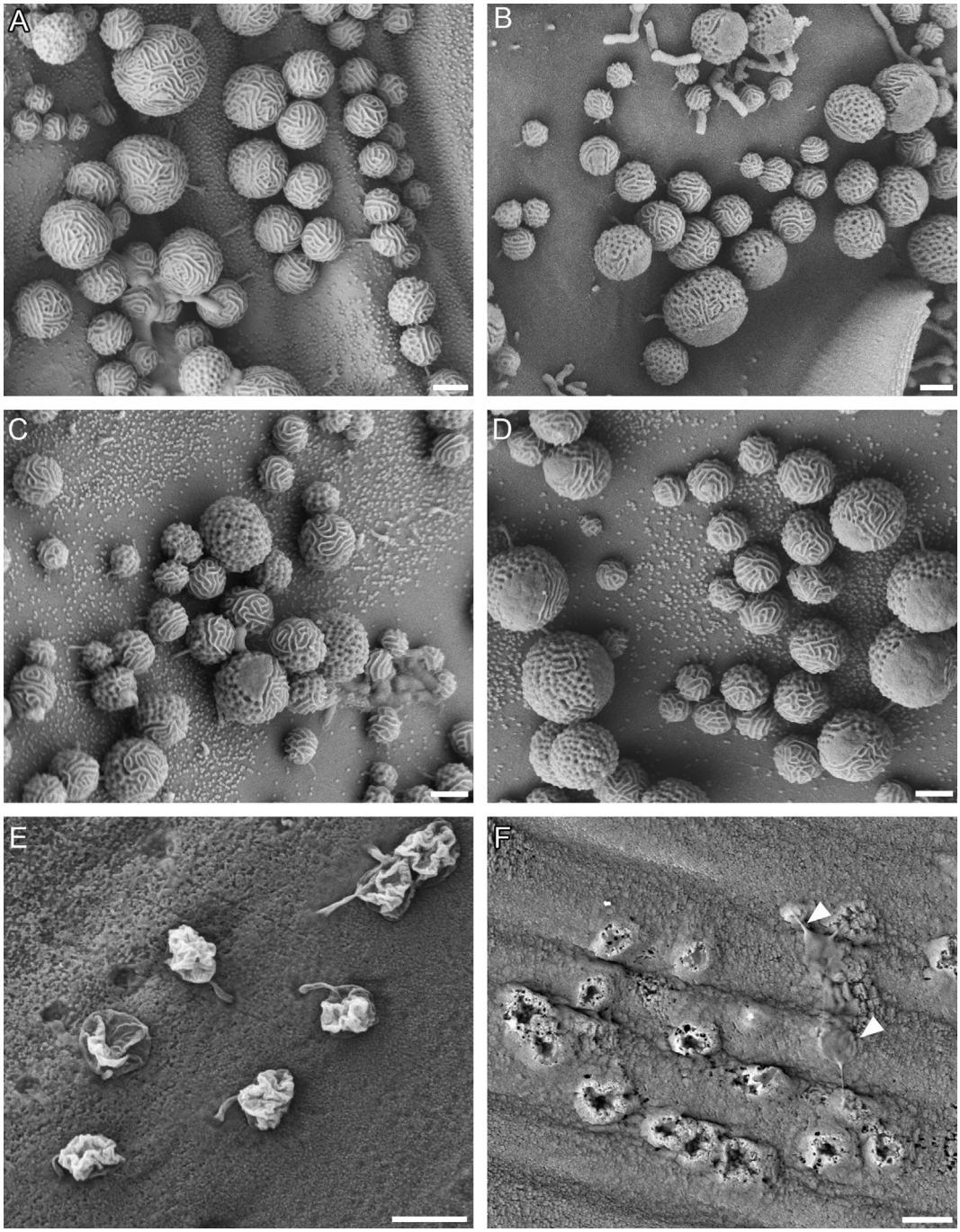

Fig. 4. Effects of exposure to different chemicals. (A) Untreated control cuticle. (B) Cuticle treated with aqueous EDTA. The granules are no longer distinguishable on the surface. (C) Cuticle treated with methanol. (D) Cuticle treated with hot chloroform. (E) Cuticle treated with aqueous NaOCl for 2 h. The spheres appear deflated and the epicuticle largely degraded. (F) Cuticle treated with aqueous NaOCl for 72 h. The spheres are removed, with only a few flattened remains (arrowheads) visible. Scale bars = 1 μm.

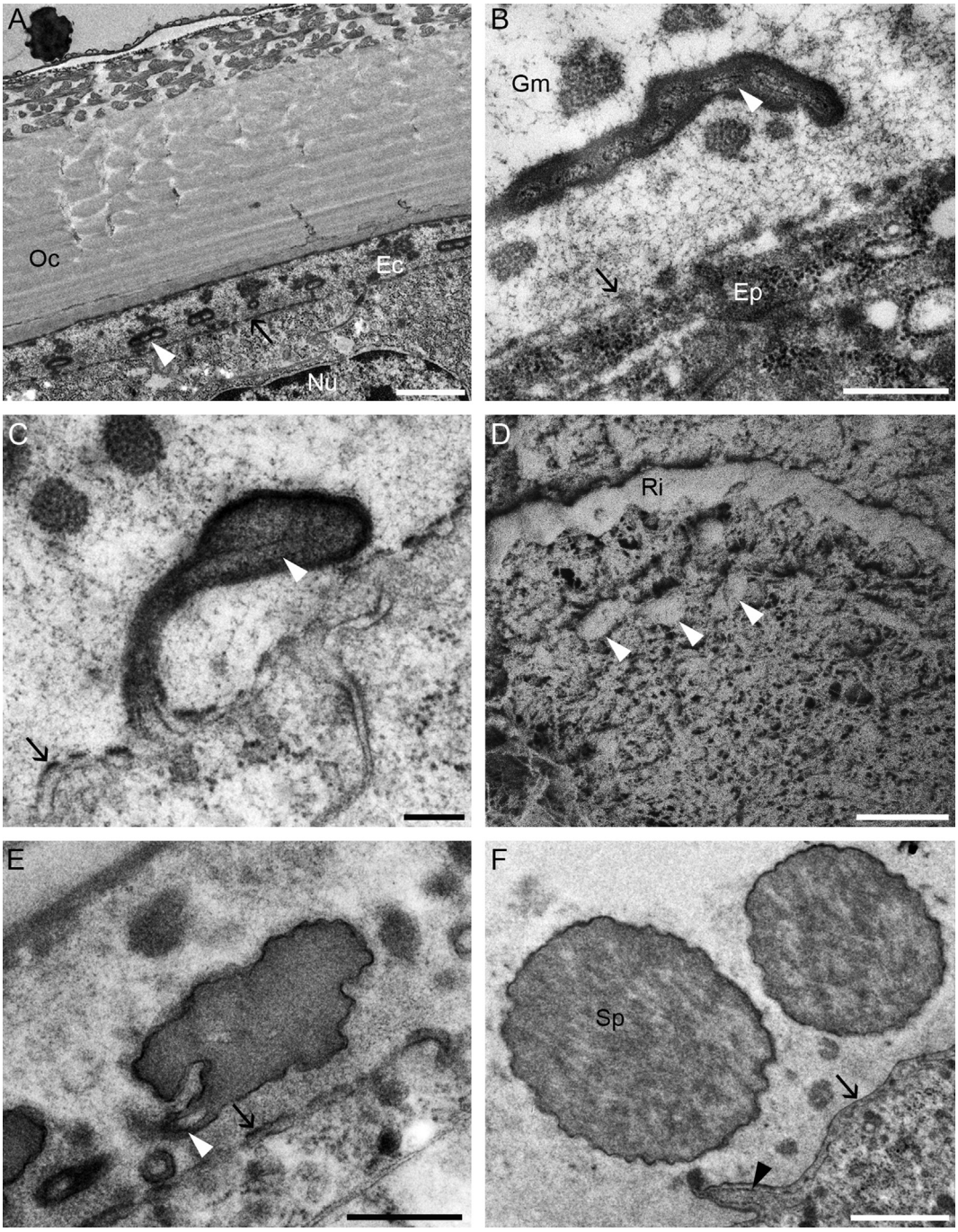

Fig. 5. Formation of spheres during the early premolt stage (PE1). (A) Transmission electron micrograph of a tergite in early premolt stage. Epidermal cells are secreting the epicuticle (arrow) and form cell extensions (arrowhead) in the ecdysial space (Ec) between the epidermis and the old cuticle (Oc). Nu: nucleus. Scale bar = 5 μm. (B) Higher magnification of the apical surface of an epidermal cell (Ep) during the early stage of epicuticular synthesis. A thin layer of electron dense material surrounds its cell extensions (arrowhead). The new epicuticle (arrow) is discontinuous. Granular material (Gm) is present in the ecdysial space. Scale bar = 0.5 μm. (C) At a slightly more advanced stage of epicuticle deposition, the dense material around cell extensions (arrowhead) thickens distally, forming a larger mass on a thinner stalk. The epicuticle (arrow) is still discontinuous. Scale bar = 200 nm. (D) Scanning electron micrograph of the epidermal surface during the early premolt stage showing the forming spheres (arrowhead) and a continuous ring (Ri). Scale bar = 2 μm. (E) At a yet more advanced stage of formation, more matrix is deposited around the cell extensions (arrowhead). The epicuticle remains discontinuous (arrow). Scale bar = 0.5 μm. (F) As the epicuticle forms a continuous layer (arrow) over the epidermis, the spheres (Sp) are round, have an inhomogeneous interior and a structured surface. The cell extensions (arrowhead) appear to retract. Scale bar = 1 μm.

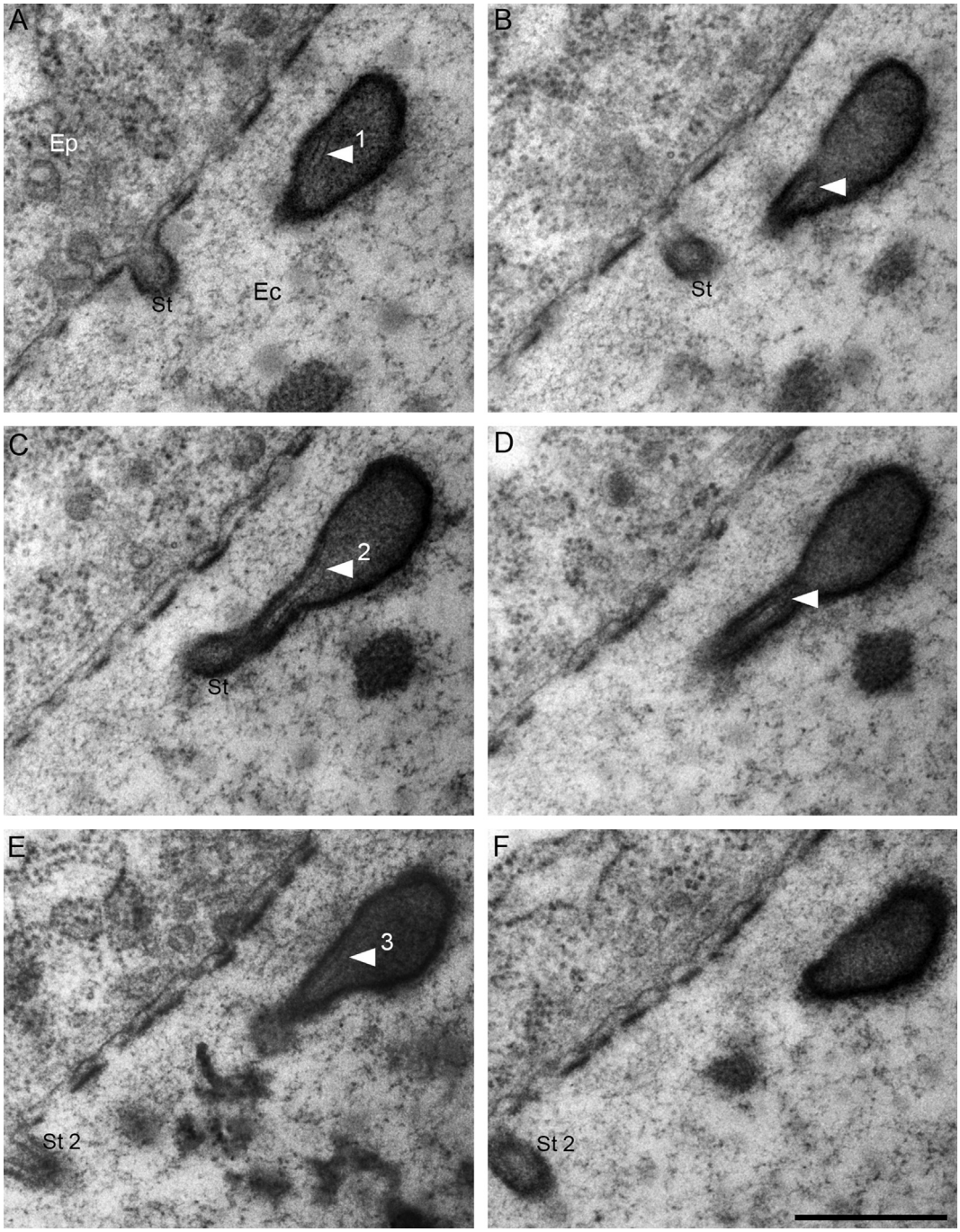

Fig. 6. Serial sections through a cell extension during the early premolt stage. Images A–F show sequential ultrathin sections. The epidermal cell (Ep) is in the process of depositing a sphere in the ecdysial space (Ec). A thickened mass of matrix is connected to the surface by a thinner stalk (St). The cell extension (arrowhead) forms a series of three parallel branches (1–3). On the last two sections, a second stalk (St 2) of the next sphere is visible. Scale bar = 0.5 μm.

This suggests that the spheres, like the rest of the epicuticle, are largely organic and sensitive to degradation by oxidizing agents. They are evidently covered with a much more durable external sheet of matrix, which is able to withstand prolonged exposure to NaOCl that rapidly degrades their interior.

3.3. Process of sphere formation

As determined with TEM, the deposition of the spheres begins concomitantly with the onset of the epicuticle secretion during the PE1 stage (Fig. 5A). Initially, the new epicuticle secreted by the epidermal cells is discontinuous (Fig. 5B). In the early stages of sphere deposition, a layer of electron dense extracellular matrix forms around extensions of the apical surface of epidermal cells. These cell extensions are around 50 nm thick (Fig. 5B and C). Each cell deposits a number of spheres by forming numerous cell extensions (Fig. 5A). As the process continues, the electron dense matrix thickens around the distal parts of the cell extensions (Fig. 5C and D). Later on, but while the epicuticle is still discontinuous, more matrix is deposited. The matrix now forms a thicker

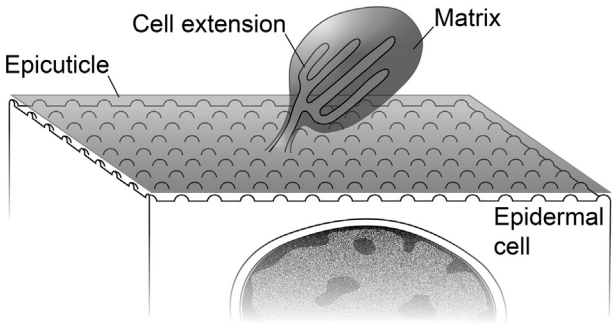

Fig. 7. Diagram of sphere formation during the early premolt stage. The matrix of a new sphere is deposited around a branching extension of an epidermal cell. For simplicity, only one extension is depicted and the epicuticle is shown as a continuous sheet.

mass on a slender stalk and its surface becomes structured (Fig. 5E). During these stages of deposition, the central matrix is less electron dense than the surface layer, which is distinguishable as a thin, electron dense layer on the surface of the forming spheres (Fig. 5C and E).

Later during the PE1 stage, the newly secreted epicuticle is continuous. The new spheres are round and have an inhomogeneous and somewhat fibrous interior with regions of varying electron density. By this time, the cell extensions are no longer distinguishable in the interior of the spheres (Fig. 5F).

As can be deduced from the observation of serial ultrathin sections, a single cell extension forms an individual sphere by forming several parallel branches, around which the matrix of the sphere is deposited (Figs. 6 and 7). As they are generally deposited by individual branching extensions, fully formed spheres are connected to the rest of the cuticular surface by a single stalk. In some cases, however, two extensions may deposit a sphere (Fig. 8A). This process likely results in spheres that have two stalks, which are often observed on the body surface (Fig. 8B). The ability of a series of cell extensions to form a continuous mass of extracellular matrix is likely the mechanism behind the formation of rings (Fig. 5D), which are consequently connected to the cuticle via several stalks (Fig. 2D).

At the onset of the deposition of the exocuticle in PE2 stage, the newly deposited spheres are indistinguishable from the spheres on the surface of the old cuticle. The material inside the spheres is inhomogeneously electron dense and their surfaces are structured (Fig. 9A and B). The stalks no longer contain cell extensions and are instead filled with extracellular matrix (Fig. 9B). No additional changes are apparent in the PE3 stage, during which the spheres appear fully formed (Fig. 9C and D).

As demonstrated by optical sectioning with structured illumination fluorescence microscopy, new spheres are not deposited a few μm posteriorly to tricorn sensilla, which form directly under the corresponding structures of the old cuticle (Fig. 10). Apart from these areas, the spheres cover the new cuticle in the characteristic periodical pattern of spheres increasing in diameter in successive rows. While the new cuticle is densely covered in spheres, the spheres on the old cuticle are sparse (Fig. 10).

3.4. Hydrophobicity of sphere-covered surfaces

The median contact angle θ between the tergite and the surface of 1 μL water droplets in powdered *P. pruinosus* individuals is 140° (the interquartile range (IQR) is 133°–146°). If the spheres are gently removed (Fig. 11A and B), the tergal surface is less hydrophobic, with a median θ of 96° (IQR = 80°–110°), a significantly smaller contact angle than in the case of powdered tergites ($p = 2.4 \times 10^{-9}$). In *P. scaber*, in which the tergal cuticle is covered in scales (Fig. 11C and D), the median θ is 116° (IQR = 107°–123°), which is significantly less than in powdered *P. pruinosus* ($p = 6.5 \times 10^{-9}$) and significantly more than in *P. pruinosus* with the spheres removed ($p = 0.003$; Fig. 11E). This demonstrates that the tergal surface in *P. pruinosus* is more hydrophobic than in *P. scaber*, the epicuticle of which forms scales instead of spheres. The observed hydrophobicity of *P. pruinosus* tergites results from the presence of spheres, as the tergal surface in *P. pruinosus* becomes less hydrophobic than in *P. scaber* if the spheres are removed.

4. Discussion

We were able to determine that the spheres which cover *P. pruinosus* are epicuticular structures deposited early in the premolt stage of the molt cycle and are fully formed prior to molt. They are mostly organic and likely consist of proteins and polysaccharides or glycoproteins. While their ultimate function is not

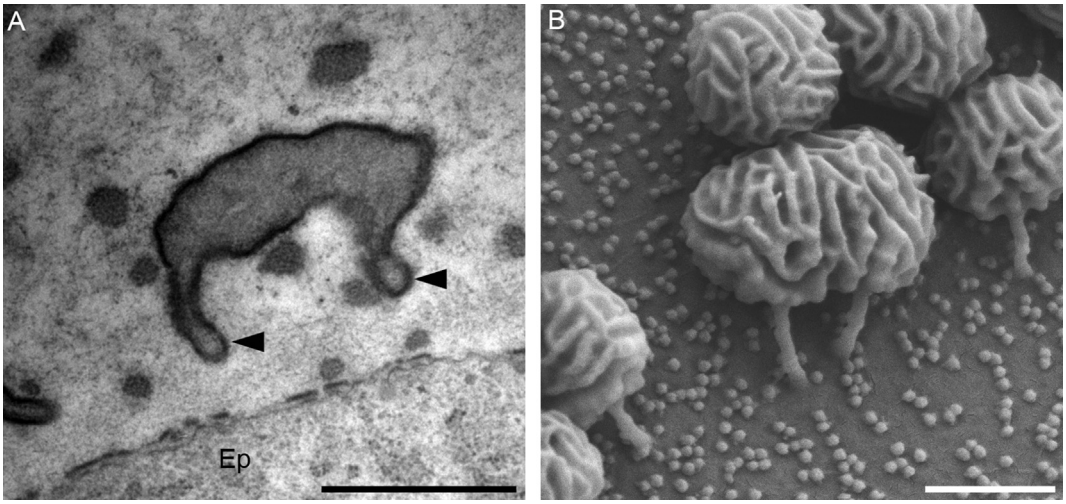

Fig. 8. Formation of spheres with two stalks. (A) Transmission electron micrograph of a forming sphere during the early premolt stage. The sphere is secreted by two cell extensions (arrowheads) of an epidermal cell (Ep). (B) Scanning electron micrograph of a sphere with two stalks on a tergite of an intermolt stage individual. Scale bars = 1 μm.

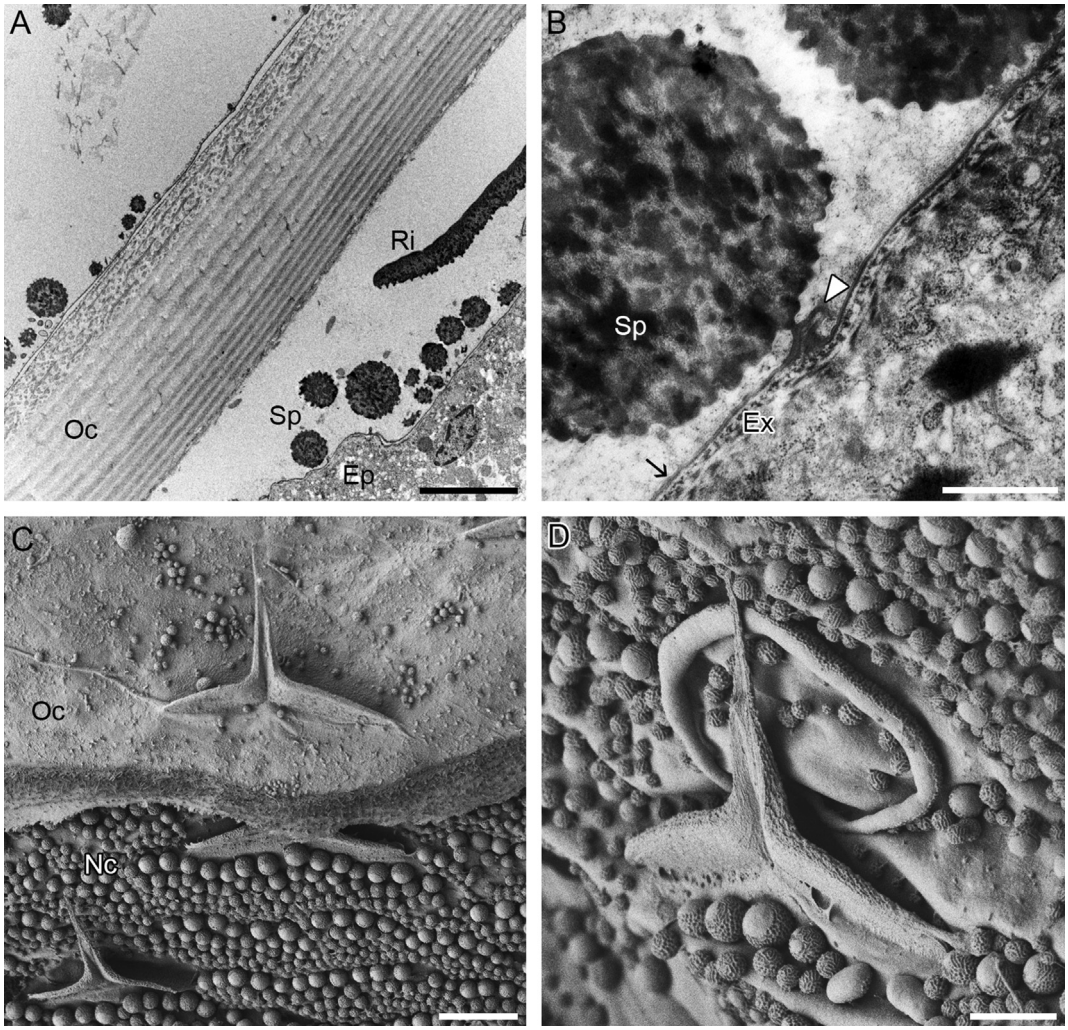

Fig. 9. Ecdysial space during the late premolt stage. (A) Transmission electron micrograph of a section through a tergite from an individual in the stage PE2. The new spheres (Sp) appear very similar to the old spheres on the surface of the old cuticle (Oc). Ep: epidermis, Ri: ring. Scale bar = 5 μm (B) Higher magnification of the surface of the epidermis during the stage PE2. The new exocuticle (Ex) is visible beneath the epicuticle (arrow). The stalk (arrowhead) of a sphere (Sp) does not contain a visible cell extension. Scale bar = 1 μm (C) Scanning electron micrograph of a tergite from an individual in the stage PE3. Numerous fully formed spheres and tricorns are visible on the surface of the new cuticle (Nc) underneath the old cuticle (Oc). The old cuticle was fractured to reveal the ecdysial space. Scale bar = 10 μm. (D) Scanning electron micrograph of the new cuticle in a specimen in the stage PE3, showing a tricorn, a ring and numerous spheres, all of which are fully formed. Scale bar = 5 μm.

known, we demonstrated that they affect the wetting of the animal by rendering its surface considerably more hydrophobic.

The spheres stain strongly with acidic dyes, such as eosin and bromophenol blue, indicating that their interior contains predominantly positively charged macromolecules. They stain positive for both amino acids and carbohydrates, indicating the presence of proteins and sugars, either as polysaccharides or parts of glycoproteins. Staining of the spheres with the PAS reaction is consistent with previous reports (Csonka et al., 2018). The spheres do not contain demonstrable amounts of lipids, which have previously been suggested as their main component (Schmalfuss, 1978). The staining characteristics of the rest of the cuticle in *P. pruinosus* are similar to those reported for *P. scaber* (Žnidaršič et al., 2018). The small relative amount of lipids in the cuticle of *P. pruinosus* has previously also been demonstrated by analysis of cuticle extracts (Quinlan and Hadley, 1983). Hadley and Warburg (1986) report that in the desert species *Hemilepistus reaumuri* and *Armadillo albomarginatus* as well as in the xeric species *Armadillo officinalis* lipids can be demonstrated by staining with Oil red O and Sudan black. However, they also report that these species possess ten times more lipids per μm^2 of cuticle than the mesic species *Porcellio laevis*, with which they compare them – a species with identical rates of cuticular transpiration as *P. pruinosus* (Quinlan and Hadley, 1983). The results of chemical exposure experiments are in agreement with the staining properties of the spheres. The spheres are apparently unaffected by exposure to hexane (Hadley and Hendricks, 1985), methanol and chloroform, which dissolve waxes and other soluble lipids. Their morphology is also not dramatically altered by decalcification with acetic acid (Hadley and Hendricks, 1985) or EDTA. By contrast, we were able to completely remove them with NaOCl together with the rest of the epicuticle, demonstrating that they are largely organic and likely proteinaceous. Nevertheless, they are remarkably durable, particularly their surface layer. This is attested by their resilience to treatment with

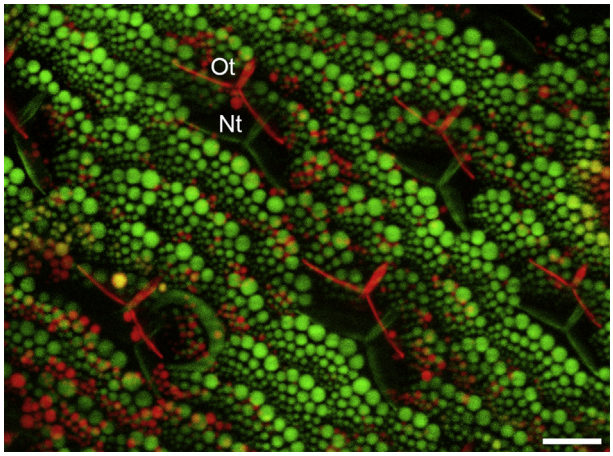

Fig. 10. Depth color-coded image of a tergite in the late premolt stage (PE3). The image is a maximum intensity projection of a stack of optical sections through the tergite. Red color represents higher structures, located on the old cuticle, whereas green color represents deeper structures in the ecdysial space. New tricorn sensilla (Nt) are formed underneath old tricorn sensilla (Ot). The spheres in the ecdysial space are much more numerous than those on the surface of the old cuticle. Scale bar = 10 μm.

10% aqueous KOH, reported by Hadley and Hendricks (1985). Considering that the spheres are epicuticular structures, their resistance to KOH treatment is not unusual. Epicuticular structures in crustaceans are known to survive KOH treatment (Krishnan, 1956) and heating in aqueous KOH is used routinely to clear crustacean exoskeletons during preparation of permanent mounts without affecting the morphology of scales and setules (Prevorčnik et al., 2012).

The spheres form during the deposition of the epicuticle. Their formation thus takes place during the s4 stage of the staging system established by Ziegler (1997) in relation to the ultrastructural changes of the integument. During the subsequent s5 stage (Ziegler, 1997), as the deposition of the exocuticle begins, the spheres are already completely formed. The entire process of their formation is thus completed during the PE1 stage of the system proposed by Zidar et al. (1998). Certain parallels can be drawn with the synthesis of epicuticular scales in other woodlice. As shown in *Titanethes albus*, epicuticular scales are deposited during the same stage and by a similar mechanism as the spheres in *P. pruinosus*. Like the spheres, the scales in *T. albus* form around cell extensions of similar thickness during the epicuticle synthesis (Vittori et al., 2012).

The assumption that the spheres and rings are deposited from the molting fluid during the postmolt stage (Hadley and Hendricks, 1985) is apparently incorrect, as they are already fully formed before ecdysis. The lack of pruinescence of the freshly molted body-half is the result of it being covered by a film of molting fluid (Fig. 1B); nevertheless, the spheres are there, and become evident as the molting fluid is removed. The spheres that were observed one on top of the other and on the tricorns (Fig. 2D, F; Hadley and Hendricks, 1985) had thus not been deposited there from the exuvial fluid, but had likely moved to these locations as a result of detachment from their stalks. On the surface of the newly formed cuticle in the late premolt stage (PE3), no spheres are visible in such places (Fig. 9). The loss of spheres leading to their repositioning on the tergal surface occurs naturally and is the likely cause of the lower density of spheres in specimens about to molt, which has been reported (Hadley and Hendricks, 1985) and was also observed in this study (Fig. 10). The proposed mechanism of ring formation by coalescence of spheres after molt (Hadley and Hendricks, 1985) is also unlikely. Transitions between circles of partly fused spheres and rings are visible on tergites in intermolt specimens as well, and are permanent states of these structures, not transient stages of their formation. Instead, fused masses of extracellular matrix are deposited in this form during the premolt stage, as demonstrated in this study.

Somewhat similar spheres have been observed on the surfaces of the related species *Orthometopon planum* (Csonka et al., 2018), *Orthometopon phaleronense* and *Orthometopon turcicum* (Schmalfuss, 1978, 1993). All of these species as well as *P. pruinosus* lack scales on their tergites, whereas scales cover the dorsal surface in the related speceis *Orthometopon dalmatinum*, which lacks spheres (Schmalfuss, 1978). These two types of surface structures are thus apparently mutually exclusive. This fact, along with the mechanism of their formation, indicates that the spheres in *P. pruinosus* are homologous to the epicuticular scales covering the tergites in related woodlice.

The results of our measurement of cuticular wettability are in favor of the hypothesis that the spheres increase the hydrophobicity of the cuticle. We naturally cannot claim that this is the ultimate cause behind their evolution, but their presence evidently results in increased hydrophobicity of the body surface. A similar function has been proposed for brochosomes of planthoppers which are also minute, finely structured spheres that cover the cuticles of the animals that produce them and render them more hydrophobic. In the case of planthoppers, a proposed function of brochosomes was not only the protection of planthoppers from liquid contaminants, such as their own excretions and plant exudates (Rakitov, 2002; Rakitov and Gorb, 2013) but also the prevention of the animals getting trapped in droplets of rain or dew (Rakitov, 2002). This could be important for *P. pruinosus* as well and has been suggested as a possible function of other surface structuring in woodlice (Schmalfuss, 1977, 1978). The tergal ridges that characterize small endogean woodlice likely reduce the adhesion of tergites to wet surfaces in the soil (Schmalfuss, 1977), which would hinder the movement of these animals in the deeper strata of leaf litter and soil. While *P. pruinosus* as a larger, more agile epigean species is unlikely to encounter similar challenges, the prevention of adhesion might be beneficial to it for other reasons. Brochosomes prevent planthoppers from sticking to liquids and spider webs due to a convenient property: they are easily removed from the cuticle (Rakitov, 2002). The same can be said for the spheres on the surface of *P. pruinosus*, which are quickly lost from the surface. Should they stick to a noxious fluid or a spider web, the animal can shed them and escape.

Another possible function of the spheres that has previously been suggested is the restriction of water loss (Hadley and Hendricks, 1985; Schmalfuss, 1978). On the basis of their unpublished observations, Hadley and Hendricks (1985) reported that cuticular transpiration was lower in pruinose *P. pruinosus* individuals than in those in which most of the spheres had been lost. A possible explanation of this effect would be that the spheres trap a layer of air close to the surface of the tergites and thus reduce the loss of water across the cuticle. Intuitively, such a function seems likely since the spheres cover the more exposed dorsal surface of the animal. However, it is unclear to us why spheres would be superior to scales in this respect. Furthermore, the rate of mass-specific water loss in *P. pruinosus* is reportedly comparable to that of other Crinocheta living in central Europe (Csonka et al., 2018; Quinlan and Hadley, 1983).

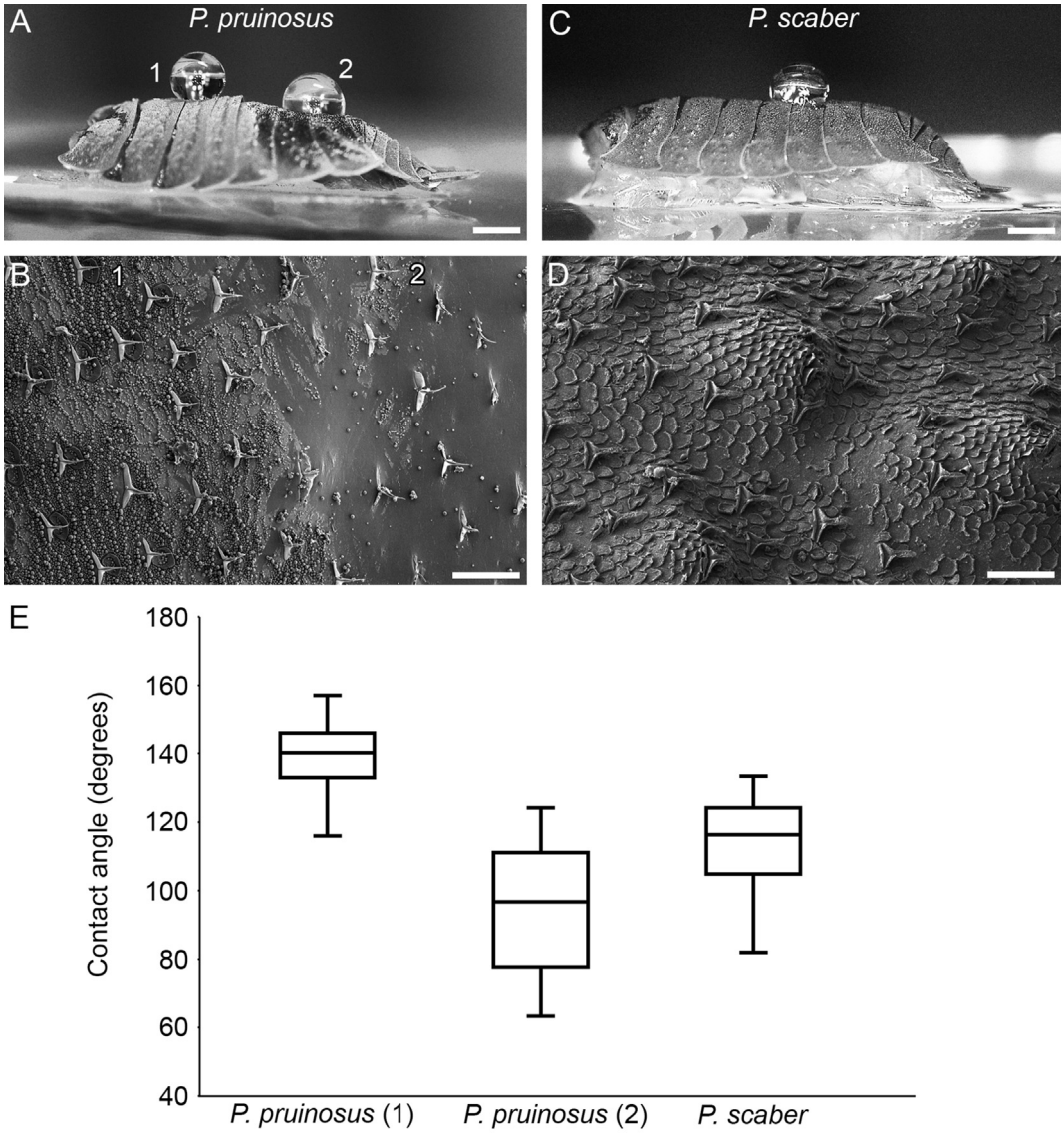

Fig. 11. Wettability of tergal surfaces. (A) Appearance of 1 μL water droplets on *Porcellionides pruinosus* tergites with spheres (1) and tergites from which the spheres were experimentally removed (2). Scale bar = 1 mm. (B) Scanning electron micrograph of a *P. pruinosus* tergite. The left side of the image shows a surface with the spheres intact (1) and the right side a surface with the spheres experimentally removed (2). Scale bar = 50 μm. (C) Appearance of a 1 μL water droplet on *Porcellio scaber* tergites. Scale bar = 1 mm. (D) Scanning electron micrograph of a *P. scaber* tergite. The epicuticle forms scales instead of spheres in this species. Scale bar = 50 μm. (E) Contact angles between water droplets and tergites in *P. pruinosus* with intact spheres (1; left), with removed spheres (2; center) and in *P. scaber* (right). Horizontal lines represent median values; boxes represent the interquartile range; whiskers represent the range of values.

Surfaces with which water droplets form contact angles greater than 150° are often categorized as superhydrophobic, whereas those with contact angles greater than 90° can be considered hydrophobic (Hsu et al., 2011). By these criteria, the pruinose cuticle in *P. pruinosus* is not superhydrophobic, but it is strongly hydrophobic, with median droplet contact angles of about 140°. The tergal cuticle of the scale-covered *P. scaber* is also hydrophobic, but much less than that of *P. pruinosus*. It is likely that the scales in *P. scaber* also reduce the wettability of the cuticular surface by trapping air and structuring the surface of the cuticle, but to a lesser extent than spheres. If the spheres are removed from the surface of *P. pruinosus* tergites, however, their hydrophobicity decreases dramatically, demonstrating that the sculpting of the surface is essential for this characteristic. As we were not able to demonstrate the presence of lipids in the spheres, this effect is likely the result of surface structuring alone.

Author contribution

MV: Conceptualization, Formal analysis, Investigation, Resources, Writing - original draft, Visualization, Supervision, IG: Conceptualization, Investigation, Resources, Writing - original draft, Visualization

Acknowledgments

The authors would like to thank Dr. Polona Mrak for her advice on histochemical techniques, Tajda Gredar for her assistance with the Schiff reagent, Jožica Murko Bulič for her laboratory assistance and Dr. Anita Jemec, Katja Lobe and Mojca Breznik for their help establishing the initial woodlouse cultures. This work was financed by the Slovenian Research Agency [Research Program P1-0184] and supported by the University Infrastructural Center “Microscopy of

Biological Samples" at the Biotechnical Faculty, University of Ljubljana.

Appendix A. Supplementary data

Supplementary data to this article can be found online at https://doi.org/10.1016/j.asd.2020.100968.

References

Bancroft, J.D., Gamble, M., 2008. Theory and Practice of Histological Techniques, sixth edition. Churchill Livingstone, London.

Csonka, D., Halasy, K., Buczkó, K., Hornung, E., 2018. Morphological traits — desiccation resistance — habitat characteristics: a possible key for distribution in woodlice (Isopoda, Oniscidea). ZooKeys 801, 481–499.

Hadley, N.F., Hendricks, G.M., 1985. Cuticular microstructures and their relationship to structural color and transpiration in the terrestrial isopod *Porcellionides pruinosus*. Can. J. Zool. 63, 649–656.

Hadley, N.F., Warburg, M.R., 1986. Water loss in three species of xeric adapted isopods: correlations with cuticular lipids. Comp. Biochem. Physiol. A Physiol. 85, 669–672.

Hammer, Ø., Harper, D.A., Ryan, P.D., 2001. PAST: paleontological statistics software package for education and data analysis. Palaeontol. Electron. 4 article 4.

Hsu, S.H., Woan, K., Sigmund, W., 2011. Biologically inspired hairy structures for superhydrophobicity. Mater. Sci. Eng. R Rep. 72, 189–201.

Kiernan, J.A., 1990. Histological and Histochemical Methods. Theory and Practice, second ed. Pergamon Press, Oxford.

Kim, S.H., Wu, S.Y., Baek, J.I., Choi, S.Y., Su, Y., Flynn, C.R., Gamse, J.T., Ess, K.C., Hardiman, G., Lipschutz, J.H., Admrad, N.N., Rockey, D.C., 2015. A post-developmental genetic screen for zebrafish models of inherited liver disease. PloS One 10, e0125980.

Krishnan, G., 1956. The nature and composition of the epicuticle of some arthropods. Physiol. Zool. 29, 324–337.

Nosonovsky, M., 2007. Multiscale roughness and stability of superhydrophobic biomimetic interfaces. Langmuir 23, 3157–3161.

Prevorčnik, S., Ferreira, R.L., Sket, B., 2012. Brasileirinidae, a new isopod family (Crustacea: Isopoda) from the cave in Bahia (Brazil) with a discussion on its taxonomic position. Zootaxa 3452, 47–65.

Price, J.B., Holdich, D.M., 1980. The formation of the epicuticle and associated structures in *Oniscus asellus* (Crustacea, Isopoda). Zoomorphology 94, 321–332.

Quinlan, M.C., Hadley, N.F., 1983. Water relations of the terrestrial isopods *Porcellio laevis* and *Porcellionides pruinosus* (Crustacea, Oniscidea). J. Comp. Physiol. 151, 155–161.

Rakitov, R.A., 2002. What are brochosomes for? An enigma of leafhoppers (Hemiptera, Cicadellidae). Denisia 4, 411–432.

Rakitov, R., Gorb, S.N., 2013. Brochosomes protect leafhoppers (Insecta, Hemiptera, Cicadellidae) from sticky exudates. J. R. Soc. Interface 10, 20130445.

Schindelin, J., Arganda-Carreras, I., Frise, E., Kaynig, V., Longair, M., Pietzsch, T., Preibisch, S., Rueden, C., Saalfeld, S., Schmid, B., Tinevez, J.Y., White, D.J., Hartenstein, V., Eliceiri, K., Tomancak, P., Cardona, A., 2012. Fiji: an open-source platform for biological-image analysis. Nat. Methods 9, 676–682.

Schmalfuss, H., 1975. Morphologie, Funktion und Evolution der Tergithöcker bei Landisopoden (Oniscoidea, Isopoda, Crustacea). Z. Morph. Tiere 80, 278–316.

Schmalfuss, H., 1977. Morphologie und Funktion der tergalen Längsrippen bei Landisopoden (Oniscoidea, Isopoda, Crustacea). Zoomorphology 86, 155–167.

Schmalfuss, H., 1978. Morphology and function of cuticular micro-scales and corresponding structures in terrestrial isopods (Crust., Isop., Oniscoidea). Zoomorphology 91, 263–274.

Schmalfuss, H., 1993. Die Land-Isopoden (Oniscidea) Griechenlands. 13. Beitrag: Gattung *Orthometopon* ('Trachelipidae'). Stuttg. Beitr. Naturkd. A 498, 1–44.

Sfenthourakis, S., Taiti, S., 2015. Patterns of taxonomic diversity among terrestrial isopods. ZooKeys 515, 13–25.

Subramoniam, T., 1982. Manual of research methods for marine invertebrate reproduction. CMFRI (Cent. Mar. Fish. Res. Inst.) Spec. Publ. 57, 1–40.

Štrus, J., Tušek-Žnidarič, M., Repnik, U., Blejec, A., Summers, A., 2019. Microscopy of crustacean cuticle: formation of a flexible extracellular matrix in moulting sea slaters *Ligia pallasii*. J. Mar. Biol. Assoc. U. K. 99, 857–865.

Vittori, M., Kostanjšek, R., Žnidaršič, N., Štrus, J., 2012. Molting and cuticle deposition in the subterranean trichoniscid *Titanethes albus* (Crustacea, Isopoda). ZooKeys 176, 23–38.

Vittori, M., Štrus, J., 2017. Male tegumental glands in the cavernicolous woodlouse *Cyphonethes herzegowinensis* (Verhoeff, 1900) (Crustacea: Isopoda: Trichoniscidae). J. Crustac Biol. 37, 389–397.

Zidar, P., Drobne, D., Štrus, J., 1998. Determination of moult stages of *Porcellio scaber* (Isopoda) for routine use. Crustaceana 71, 646–654.

Ziegler, A., Fabritius, H., Hagedom, M., 2005. Microscopical and functional aspects of calcium-transport and deposition in terrestrial isopods. Micron 36, 137–153.

Ziegler, A., 1997. Ultrastructural changes of the anterior and posterior sternal integument of the terrestrial isopod *Porcellio scaber* Latr. (Crustacea) during the moult cycle. Tissue Cell 29, 63–76.

Žnidaršič, N., Mrak, P., Rajh, E., Žagar Soderžnik, K., Čeh, M., Štrus, J., 2018. Cuticle matrix imaging by histochemistry, fluorescence, and electron microscopy. Resol Discov 3, 5–12.